Real Time Color Purity and Convergence Measurement Algorithms for Automatic ITC Adjustment System

Zeungnam Bien, Dongil Han, Jongcheol Park, Jong-Woon Lee
Department of Electrical Engineering
Korea Advanced Institute of Science and Technology
373-1 Kusongdong, Yusongku, Taejeon, 305-701 Korea

Changsuk Oh
Production R & D Center
Samsung Electron Devices
575, Sinri, Taean, Hwasung, Kyungki, 445-970 Korea

Abstract

In manufacturing CPT(Color Picture Tubes) used in TV sets and monitors, an ITC(Integrated Tube Components) adjustment process is involved. The adjustment process requires expertise and human fatigue, and thus is considered to be a bottleneck in enhancing productivity of CPT manufacturing. Automating the ITC adjustment process needs fast and robust visual sensing/measurement. In this paper, real time color purity and convergence measurement algorithms are described. Existing color purity measurement algorithms for ITC adjustment system often take too much time to detect color purity. Moreover, for convergence measurement, measurable data is not sufficient for accurate detection. To overcome these difficulties, real time vision system with 9 area cameras and many linear array cameras is developed. Area cameras are used for color purity measurements and linear array cameras are used for convergence measurements.

To devise the purity measurement algorithm, the characteristics of CPT microscopic images are analyzed. To measure the exact color purity, several methods are selectively applied for calculating color purity depending on the conditions of CPT screen. For convergence measurement, special test CPT with no shadow mask and no black matrix is manufactured and a new measurement algorithm is developed using fuzzy inference and a priori *knowledge taken from the specially manufactured CPT. The proposed algorithms are successfully applied as described in the experimental results.*

1 Introduction

As the need for mass production and high quality is increasing, the need for automation of industrial processes is increasing. ITC(Integrated Tube Components) adjustment process is an example of such a system[1]. ITC adjustment is an essential process in manufacturing color picture tubes(CPT). This process includes the adjustment of focus, tilt, brightness, color purity, and convergence of three electron beams(Red, Green, and Blue beams)[2].

Thus far, the adjustment and the inspection of CPT are done manually by human experts. In this case, the quality of the whole process is determined by human operators. It is very difficult, however, to manually adjust CPTs, such as HDTV and computer graphics terminal, which require large-size CPT or very high resolutions since they are hard to handle with[3]. In many cases, the inspection depends heavily upon the operators judgement which may vary with fatigue, experience and eyesights. And operator's fatigue and variations between operators make it difficult to guarantee consistent inspection and adjustment quality.

As CPT manufacturers strive for higher standards of product quality, it is founded that traditional testing and control procedures are too slow, too inconsistent and too resistant to statistical analysis. Hence the need for the automated adjustment system arises. That is, in order to enhance the productivity and the uniformity of product's quality, it is required to automate the ITC adjustment process[4] and the automation requires real time vision system for inspection and measurement.

This paper describes the design of a multiprocessor-based automatic measurement system for ITC process. Section 2 describes the structure of Color Picture Tube, section 3 describes the purity measurement algorithm and section 4 describes the convergence measurement algorithm. Section 5 shows the experimental results and conclusion follows in section 6.

2 The Overview of ITC Adjustment System

Color Picture Tube(CPT) generally consists of three(red, green, blue) electron guns, a shadow mask, a phosphor screen, a glass bulb. And it also include Convergence and Purity Magnet rings(CPM) and Deflection Yoke(DY), which are located at the rear part of CPT. Fig. 1 shows the structure of a CPT. DY supplies the vertical and horizontal magnetic fields so that the spatial trajectories of electron beams are deflected according to the synchronization signals. Three electron beams emitted from R.G.B electron guns are controlled, focused and accelerated by a set of grids of each electron gun. It then becomes deflected by the DY attached to the Funnel Glass Cone and CPM on the neck. Electron beam converges on one hole of slot type shadow mask which is 5-15mm apart from panel glass, and collides with corresponding phosphor, and then emits light. That is, in the case of red beam, it is desired to collide with only the red phosphor and emits red light, green beam the green phosphor and blue beam the blue phosphor.

The arrangement of electron guns, shadow mask,

0-8186-2840-5/92 $03.00 © 1992 IEEE

and phosphor stripes is shown in Fig. 2. The phosphor screen consists of black matrix(BM) and three phosphor stripes, red, green, and blue phosphor stripes. black matrix is a black light absorbing material to absorb the outer-light on screen and improves contrast on CPT. The electron beams emitted from the electron guns hit the phosphor screen through the mask hole. The phosphor screen hit by electron beam emits light.

When the three electron beams reach a precise spot on the phosphor screen, the luminous light becomes pure. Purity points to the purity of this luminous light. In other words, color purity is determined by the correct landing of R,G,B beams on their phosphor. If the three electron beams emitting from the electron gun fail to make a correct landing on the corresponding phosphors, or if the flights of beams are affected by such an external magnetic field as the terrestrial field, colors of the screen image will be of low purity, especially in the periphery of the screen. It is determined by the interrelation between electron gun, shadow mask, and phosphor stripe of CPT.

To realize a vivid color in color CPT, the convergence of each beam is indispensable. Convergence means the concentration of three R.G.B electron beams towards a certain point in shadow mask hole as shown in Fig. 2. Due to variation of the parts characteristics and mismatches in manufacturing process, the purity and convergence may be not in good condition at first. To compensate this, CPM, consisting of 2 pole, 4 pole and 6 pole permanent magnetic rings, are devised and they have the capability of modifying the electron beam trajectories locally. ITC adjustment process is mainly manipulating this 6 CPM rings(each pole pair) and z-axis position and orientation of DY to realize a good quality image on screen. Purity is adjusted by the rotation of 2 pole CPM and z-axis linear motion of DY. Static convergence is adjusted with 4 pole and 6 pole CPM; while dynamic convergence is by pull and back of DY. Here, the three beams must converge in whatever hole of the shadow mask. In case of poor convergence, there will be color blurring or blooming and thus color image on screen may be not clear. For example, we can see the red edge of white flower in old color television set occasionally. If the red, green, blue electron beams get the same landing position or/and pass through the same shadow mask hole, the dummy color of image, like the red edge of white flower, does not exist.

3 Purity Measurement Algorithm

3.1 Features of CPT screen image

The human inspector determines the CPT conditions by examining the shape of the luminous phosphor with magnifying lens. The luminous area of CPT screen is the luminous phosphor which is the intersection of the phosphor stripe and electron beam. The CPT conditions can be classfied into 9 types. For A type, the center of phosphor coincides with that of electron beam. Depending on the distance between two centers, they are further classified into B, C, D, and E type. Here the difference of real landing errors between these types of images is approximately 15 μm for 29" CPT case. Tipically, the width of phosphor stripe is about 170 μm. In the A, B and C types, the width of luminous phosphor is the same as that of phosphor stripe. In the D type, one side end of electron beam illuminates inside of the phosphor. In this case, the brightness of CPT is dark because some part of the electron beam hit the Black Matrix(BM) for which the phosphor is not coated and the width of luminous phosphor is smaller than that of phosphor stripe. In the E type, the electron beam illuminates the two kind of phosphors simultaneously. For example, the *green* electron beam hits green phosphor and red phosphor simultaneously, which causes the stain in the screen. In addition to the 5 conditions, there are also R type and L type to be classified. $R(ight)$ type means that electron beam is deflected to the left side of phosphor, and $L(eft)$ type means that electron beam is deflected to the right side of phosphor. All the types of images are depicted in Fig. 3.

Some features that can be used for classification of CPT conditions are depicted in Fig. 4. The area of luminous phosphor is a feature that may be used for classifying several CPT conditions. It attains maximum in A type case. The area becomes smaller as the distance between the center of phosphor and that of electron beam becomes larger. But because the area can not tell R type and L type and also is sensitive to the width of phosphor which varies according to CPT's, the area is not used as a feature information in our algorithm.

Instead, the width of luminous phosphor and the shape of lower and upper curves are adopted as feature information. The width of luminous phosphor is varying depending on types. Therefore it is used to differentiate D and E types from A, B and C types. The shape of lower and upper curves renders a good information for classifying all types of CPT conditions. In our algorithm, the width of luminous phosphor is used for classifying D and E types and the shape of curves is used for classifying A, B and C types.

3.2 Purity measurement algorithm

For an on-line puruty measurement, high speed image processing that is robust to noise, is desired. We propose an algorithm with such characteristics whose flow chart is shown in Fig. 5. Detailed description of each block is described as follows.

3.2.1 Binarization and window setup

For fast image processing, binary images are used for purity measurement. In the off-line stage, a threshold level is determined to obtain binary images based on the concept of a separability function[5]. Such a calculated threshold level is directly used also at the on-line stage with lookup table.

Even with binarization, the processing time for all 512×512 pixels takes a lot of time but can be reduced by windowing. The size of window is determined on-line by the width and length of luminous phosphor.

3.2.2 Purity measurement for E type image

Prior to purity measurement, we must examine the beam conditions in the selected window. The binarized image in the window is sampled and the CPT condition is E type if there are rows having two luminous phosphors. Denote $w(x, y)$ as a charateristic function whose value is one for an image point corresponding to the luminous phosphor and zero for the points on the Black Matrix and nonluminous phosphors in the window. Then as shown in Fig. 6, the vertical projection function $v(x)$ is defined as

$$v(x) = \int_{y_0}^{y_1} w(x, y)dy. \tag{1}$$

For E type case, two clusters are found in the $v(x)$ profile and they can be represented as $c_1(x)$, $c_2(x)$ as shown in Fig. 6. Denoting the two ordinates of the peak positions of each cluster as q_1 and q_2, respectively, we find intervals in which $v(x)$ exceeds a given threshold level, and the boundary positions p1, p2, p3, and p4 of the intervals are calculated as follows.

$$p_1 = min\{x : x < q_1, c_1(x) \geq c_1(q_1)/2\} \tag{2}$$

$$p_2 = max\{x : q_1 < x < q_2, c_1(x) \geq c_1(q_1)/2\} \tag{3}$$

$$p_3 = min\{x : q_1 < x < q_2, c_2(x) \geq c_2(q_1)/2\} \tag{4}$$

$$p_4 = max\{x : x > q_2, c_2(x) \geq c_2(q_1)/2\} \tag{5}$$

The center positions of beam and phosphor stripe can be calculated as follows.

$$center_{beam} = (p_1 + p_4)/2 \tag{6}$$

$$center_p = \begin{cases} p_2 - width_p/2\ , & if\ (p_2 - p_1) > (p_4 - p_3) \\ p_3 + width_p/2\ , & if\ (p_2 - p_1) < (p_4 - p_3) \\ Undetermined\ , & otherwise. \end{cases} \tag{7}$$

The width of phosphor stripe is needed in calculating the purity. For E type, the width of phosphor stripe can not be measured because only a part of phosphor stripe is hit by the electron beam. In that case, backup data calculated at the off-line stage or design specification is used as a width of phosphor stripe, or the measured width at A, B or C type cases can be used. If $(p_2 - p_1) \approx (p_4 - p_3)$, we determine the exact beam center position by using the result calculated at other positions of CPT screen. Then the landing error δ can be calculated by subtracting the center value of the electron beam from the center value of the phosphor stripe as follows.

$$\delta = center_p - center_{beam} \tag{8}$$

3.2.3 Purity measurement for D type image

To detect whether the beam condition is of D type or not, we must compare the width of luminous phosphor with *a priori* known width of phosphor stripe. If the width of luminous phosphor is smaller than that of phosphor stripe, we conclude that th condition is D type. Otherwise, we can conclude that the CPT condition is A, B or C type. To measure the landing error at D type case, we must know the width of electron beam as in the case of E type. The method of calculating the landing error is described as follows.

As in the case of E type, the vertical projection is used to calculate the $v(x)$, and p_1 and p_2 can be calculated as shown in Fig. 7, DL type and DR type is determined using the value of $v(x)$ at the positions of p1 and p2. If $v(p_1)$ is smaller than $v(p_2)$, the CPT condition is R type and vice versa. The center position of the beam and the center position of the phosphor stripe can be calculated as follows.

$$center_{beam} = \begin{cases} p_1 + width_{beam}/2\ , & if\ R\ type\ case \\ p_2 - width_{beam}/2\ , & if\ L\ type\ case \end{cases} \tag{9}$$

$$center_p = \begin{cases} p_2 - width_p/2\ , & if\ R\ type\ case \\ p_1 + width_p/2\ , & if\ L\ type\ case \end{cases} \tag{10}$$

Then the landing error δ can be calculated by subtracting the center value of the electron beam from the center value of the phosphor stripe as follows.

$$\delta = center_p - center_{beam} \tag{11}$$

3.2.4 Purity measurement for A, B, C type images

For A, B, and C types, the width of luminous phosphors are the same but images have different shapes of curves at the upper part and lower part of the luminous phosphor. In these cases, we can find the landing error δ using vertical projection. The x-coordinate of center of mass only is needed for calculating the landing error, and so let $(x_i, y_i), i = 1, ..., n$ be replaced by $(x_i, v(x_i)), i = 1, ..., n$ as shown in Fig. 8. Then the x-coordinate of center of mass, X_c is defined by

$$X_c = \frac{\sum_{i=1}^{n} x_i v(x_i)}{\sum_{i=1}^{n} v(x_i)} \tag{12}$$

Here, X_c becomes the center axis of the electron beam of ideal symmetric curve. The landing error δ can be calculated by subtracting X_c from the center of phosphor stripe.

$$\delta = (p_1 + p_2)/2 - X_c \tag{13}$$

4 Convergence Measurement Algorithm

4.1 Conventional Convergence Measurement Methods

Convergence is practically measured from the correspondence of the three color cross stripe patterns. Therefore, in ITC process, human expert inspects the cross pattern in CPT and if three color of cross pattern are seen as a single white line at CPT, then we say that the convergence of CPT is good.

There are many research efforts trying to measure the convergence automatically. But it is not easy to measure the convergence in real time, since the output cross pattern image is sampled inherently by shadow mask and black matrix. The phosphor and black matrix configuration is shown in Fig. 9. In case of cross pattern, about five phosphors per one color stripe emit light. This is not enough for asymmetric curve fitting. Actually most of beam is invisible because of the black matrix and other color phosphors. We can see only about 20 percentage of beam for one color. To estimate the center of beam, human expert guess the cross pattern intensity profile using *a priori* knowledge, sampled data profile and the trend of data variation due to the adjustment action.

There are two method for measuring color convergence. One is the deflection method that the electron beam is deflected intensionally using small magnetism in order to know the real electron beam position. In this method, several measurements are required to estimate the pattern width and maximum intensity position. Therefore this method takes too much time for real time convergence measurement. Moreover, since the lens of linear image camera has some blurring effect and nonlinear characteristics, there exist inherent errors in measurement.

The other methods which needs only one measurement is the center of gravity method and the curve fitting method. However, if we use these method for the estimation of real maximum peak position, it contains large error(about ± 300 μm).

In this paper, a new fuzzy estimation method with only one measurement is proposed. For practical implementation, we have developed a color linear imaging system. The color linear imaging system is more efficient in time and memory requirements than the 2-dimensional color imaging system. The linear imaging system has a 1-dimensional photosensor array to acquire the essential image and has high resolution. Fig. 10 shows the example of linear array data obtained by the color linear imaging system without sampling effects due to shawdow mask and black matrix. Fig. 11 shows the image intensity profile which is not sampled. The intensity profile in cross pattern is asymmetric and nonlinear. This data is acquired from the specially made test CPT which has no black matrix and no shadow mask. Consequently, a simple curve fitting is not feasible for the beam center estimation and human decision with adjustment action is used for the estimation of beam position. therefore, a new method using fuzzy estimation algorithm for the convergence measurement is proposed and implemented.

4.2 Fuzzy Convergence Measurement Algorithm

We propose here the estimation algorithm to find the maximum intensity position and width using fuzzy inference with only one time measurement and *a priori* knowledge. For *a priori* knowedge acquisition, a special test CPT was made and the intensity profile of cross pattern was observed for many case. We must guess the intensity profile at invisible range for precise measurement. If the cross pattern of three color has maximum intensity at the same position and same beam width, we can conclude that the CPT has the good convergence. To estimate the maximum intensity position and line width, a fuzzy inference is used and the fuzzy rules are extracted from the following procedures. First, in order to know the unsampled intensity profile, we made a test CPT which has not shadow mask and black matrix. Then, the data obtained from the test CPT is analyzed and then the features of curve are extracted. Secondly, we investigated the sensing behavior of human experts. Usually, human expert recognize cross pattern of the each color using the sampling pattern intensity profile and the variation due to CPM adjustment. From these observations, we made fuzzy rules and applied them to estimate the cross pattern position.

The useful image feature for convergence measurement is as follows;

$$L_p = \frac{L\_peak}{Max\_Peak} \tag{14}$$

$$R_p = \frac{R\_peak}{Max\_Peak} \tag{15}$$

$$Peak\_Diff = R_p - L_p \tag{16}$$

$$ES = \frac{E_p - E_{p2}}{Max\_Peak} \tag{17}$$

$$EI = \frac{Ep}{Max\_Peak} \tag{18}$$

Max_Peak : The maximum intensity of linear array image data acquired.
L_p : The left next peak from the maximum peak.
R_p : The right next peak from the maximum peak.
E_p : The edge peak intensity of a bundle of peaks.
E_{p2} : The next peak from the edge
The real maximum peak of the beam is usually between the maximum peak and the right peak or the left peak. Since the intensity profile is asymetric, we make the rules which contain the asymetric characteristic of beam profile.

R1 If Peak_Diff is **Positive**, then the real peak is located **More Left**.

R2 If Peak_Diff is **Negative**, then the real peak is located **More Right**.

When the Peak_Diff is small, the R1 and R2 are dominant. However, in case of large Peak_Diff, these rules are not suitable. Therefore, for the large Peak_Diff, another fuzzy rules are required as follows.

R3 If L_Peak is **Large**, then the real peak is located **More Left**.

R4 If R_Peak is **Large**, then the real peak is located **More Right**.

For the large Peak_Diff, we made R3 and R4. And the fuzzy rule for real width estimation are as follows;

R5 If the ES is **Steep** and the EI is **Bright**, then the width is **Wide**.

R6 If the ES is **Steep** and the EI is **Dark**, then the width is **Narrow**.

R7 If the ES is **Not Steep** and the EI is **Bright**, then the width is **Medium**.

R8 If the ES is **Not Steep** and the EI is **Dark**, then the width is **Narrow**.

We made the observations into the fuzzy rules for the asymmetric property of beam intensity profile and behavior of human perception. To estimate the real beam width, the fuzzy inference is carried out for left and right edge with same rules. These rules and membership functions are constructed using the previous observations and experiments. The Simple Sugeno Implication method[6] is used for fuzzy inference.

The overall flowchart of convergence measurement is shown in Fig. 12. First, linear array image is acquired from the Color Linear Imaging System which is developed for ITC adjustment system. Second, nonlinearity of sensor is compensated and the effective data is extracted. Third, the image feature is extracted from the effective linear image data. And then, the position of maximum intensity and the width of cross pattern is taken by fuzzy inference using image feature. The differences among the center of three color pattern is transfered to the convergence adjustment system. The CPM is adjusted using this difference. And if the position of maximum peak of the three color are aligned within error tolerance and the stripes of the three colors are fully overlapped, then convergence adjustment of CPT is fulfilled.

5 Experimental Results

The proposed algorithms for color purity and convergence measurement were applied to a machine developed for CPT adjustment system. The block diagram of the developed CPT adjustment system is described in Fig. 13. The system consists of one MC68030-based supervisory controller, five MC68030-based vision data processors with a coprocessor MC68882 for fast processing of image data and a set of vision unit. The vision unit consists of five Frame Grabbers, nine cameras and five monitors. It takes charge of sensor part of overall system. One Frame Grabber interfaces with one camera which captures image at the center part of CPT. The other four Frame Grabbers interface with two cameras each which captures the images at the corner parts of CPT. Each five data processor processes the image data acquired from one Frame Grabber.

In order to acquire the information which is necessary for control unit, vision system captures the CPT images from nine cameras and processes the captured images using selected algorithms and transfers the calculated landing values to the control unit. And also, it displays the landing conditions of CPT screen using monitors. Frame Grabber captures 512 × 512 digitized images. Each pixel has 256 brightness levels. Each camera lens has same magnification factor, and magnification factor is experimentally determined so that 6 ~ 9 pixels of CPT can be stored in one frame image at any point of CPT. So, 1 pixel has the width of 4.8 μm in the real space. Each Frame Grabber has 8 Look-up Tables for efficient and fast processing.

To measure the landing values, different algorithms proposed in Section 3 are used for each types of CPT condition. If the width of luminous phosphor is the same as *a priori* known width of phosphor stripe, the algorithm for A ~ C type condition is selected and then the landing value can be calculated using selected algorithm. If two clusters of phosphor are found in the selected window, the algorithm used at the E type condition is selected and the landing value is calculated with different methods. Fig. 14 ~ Fig. 18 show the measurement results of each types of CPT images with 100 experiments. As shown in several figures, the variation of landing value measured at the A type case shows smallest dispersion and the range of dispersion is less than 6 μm. The dispersion of landing value measured at the D type and E type is similar to that of A type case. For B and C type case, the dispersion of landing value is somewhat larger but most of measured landing values range within 10 μm. From these results, we can conclude that the measurement error becomes smaller as the distance between two centers becomes smaller. All processing time needed to calculate landing value from image capturing is 480 *msec* for A, B, C, and D type cases and 390 *msec* for E type case.

In convergence measurement, the positions of maximum intensity and the widths of each color pattern using fuzzy inference are shown in Fig. 19. It also shows the curve fitting result. From the curve fitting, we find that the estimated peak appeared around the second maximum peak. It is clearly observed from the test CPT that the maximum peak of real beam is not here. However, the estimated maximum peak from the fuzzy inference appeared nearby the maxmum peak. The proposed method was heuristically evaluated by human sense and deflection of magnetism. According to the experimental result, the proposed method is better than conventional method in most of the cases and it takes more reasonable value for convergence adjustment. It is our next aim to evaluate the error between the real line and the estimated line.

6 Conclusions

A real time vision system and algorithm for an automatic adjustment system for ITC process was described. The possible features of CPT screen images are analyzed in detail and a feasible real time purity measurement algorithm was suggested. Several features are selectively used for calculating color purity depending on the conditions of CPT screen. The key feature of convergence measurement algorithm is

a fuzzy inference using insufficient amount of data with *a priori* knowledge. The estimated pattern using fuzzy logic is more similar to the unsampled real cross pattern than the one obtained from conventional method. As a result, if we have only small on-line information to make a decision, then it is found that a prior knowledge is very useful and it can be effectively used with fuzzy inference for valuable information extraction. The proposed algorithms are successfully applied and are regarded useful for microscopic measurement of automation system.

References

[1] S. Uno, et al., "Automatic Evaluation System for CPT Picture Characteristics," *Proceedings of IECON* '84, pp.432-437, 1984.

[2] T. Hibara, et al., "Automatic Adjustment for Color Display Monitor," *Proceedings of IECON* '86, pp. 164-169, 1986.

[3] A. Nakamura, et al., "Display Monotor Intelligent Adjustment System : DIAS," *Proceedings of IECON* '89, pp.715-720, 1989.

[4] Z. Bien, et al., "Development of an Automatic Adjustment System for Integrated Tube Components," *Proc. IEEE Rob. and Auto. Conf.*, pp. 993-998, May 1992.

[5] H. Otsu, "A Threshold Selection Method from Gray Level Histogram," *IEEE Trans. Syst. Man Cyber.*, vol. **SMC-9**, pp. 62-69, 1979.

[6] C. C. Lee, "Fuzzy Logic in Control Systems : Fuzzy logic Controller-Part I," *IEEE Trans. Syst. Man Cyber.*, vol. **20**, no. 2, pp. 404-417, 1990.

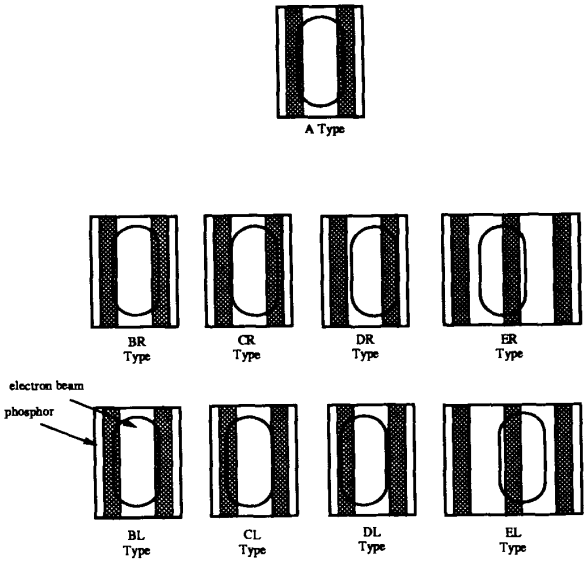

Fig. 3. Landing condition at the center part of CPT.

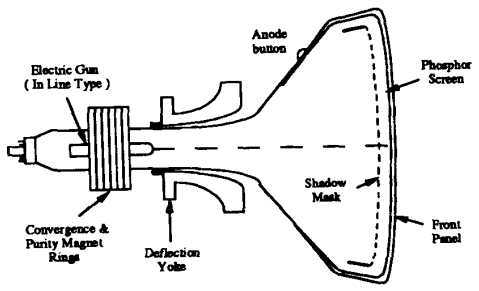

Fig. 1. The structure of Color Picture Tube.

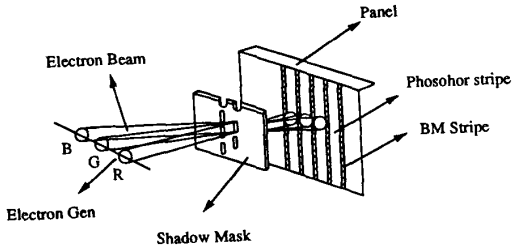

Fig. 2. The arrangement condition of electron guns, shawdow mask and phosphor stripes.

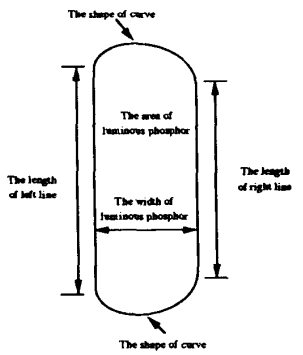

Fig. 4. The features of luminous phosphor.

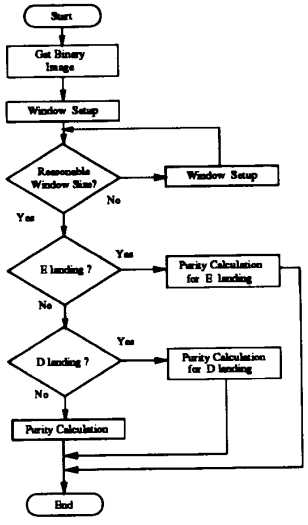

Fig. 5. The purity measurement algorithm.

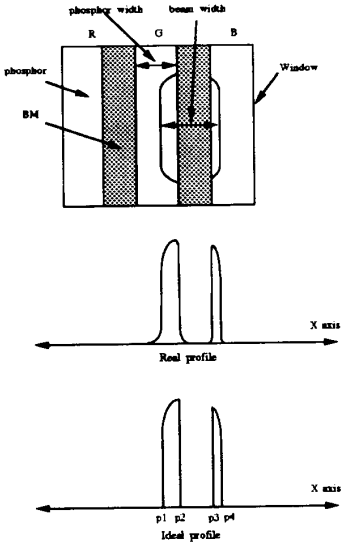

Fig. 6. The case of E type image.

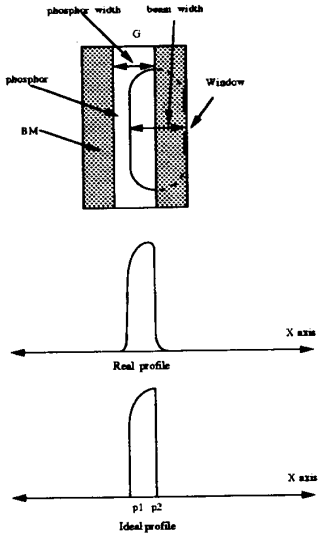

Fig. 7. The case of D type image.

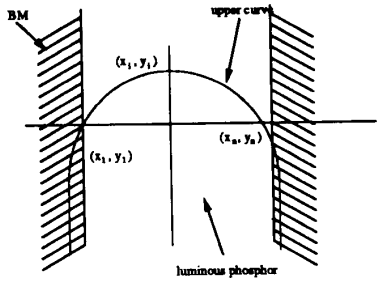

Fig. 8. The case of B type image.

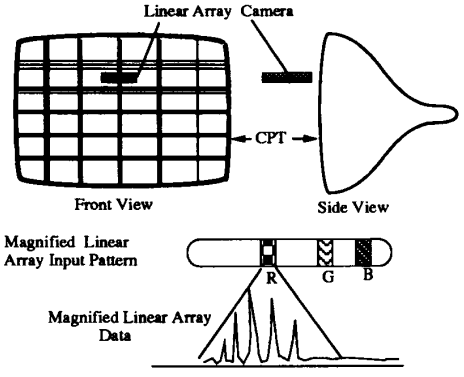

Fig. 9. Convergence Measurement Configuration

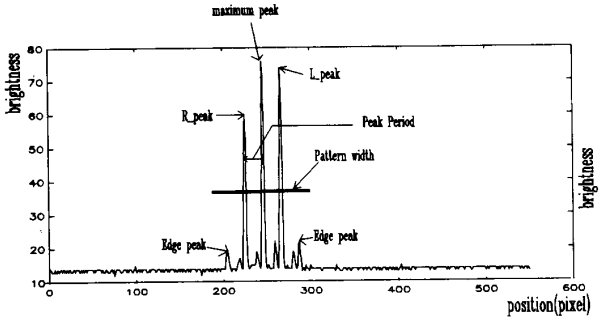

Fig. 10. The example of linear array data.

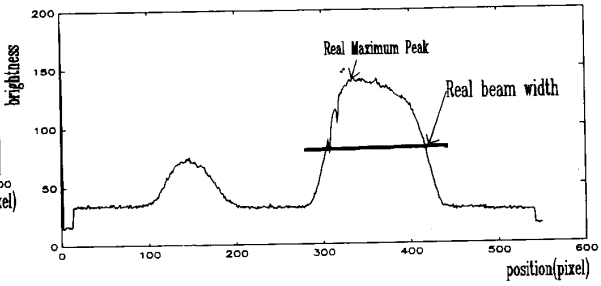

Fig. 11. The linear array data without shadow mask and black matrix.

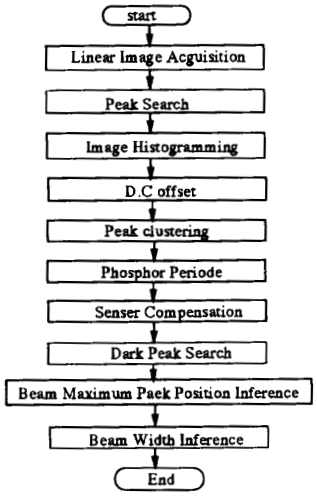

Fig 12. Convergence Measurement Algorithm Flow Chart.

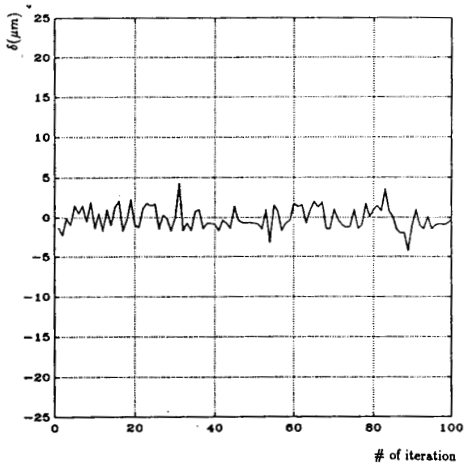

Fig. 14. The measurement result at the A type image.

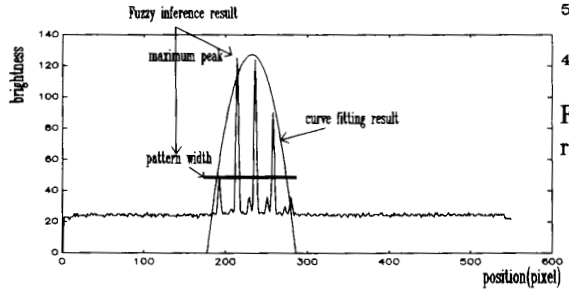

Fig. 19. The fuzzy peak and width estimation result.

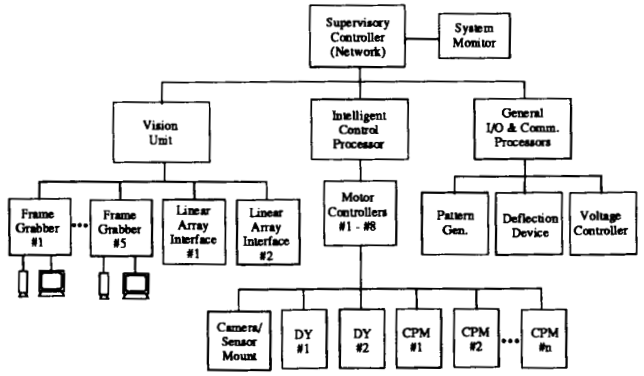

Fig. 13. The block diagram of CPT adjustment system.

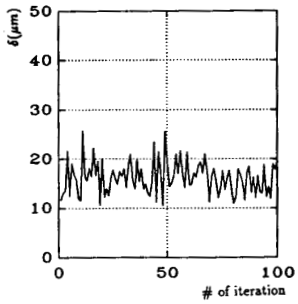

Fig. 15. The measurement result at the B type image.

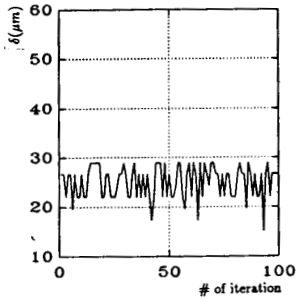

Fig. 16. The measurement result at the C type image.

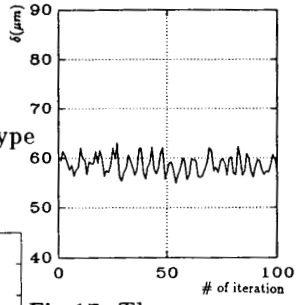

Fig 17. The measurement result at the D type image.

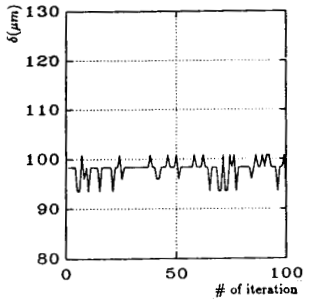

Fig 18. The measurement result at the E type image.